Hindawi
Geofluids
Volume 2022, Article ID 2697311, 11 pages
https://doi.org/10.1155/2022/2697311

Research Article

Unsteady Productivity Prediction for Three-Dimensional Horizontal Well in Anisotropic Reservoir

Gang Bi,[1,2] **Ying Cui**,[1,2] **Jiemin Wu**,[1,2] **Zongxiao Ren**,[1,2] **Fei Han**,[1,2] **Xin Wang**,[1,2] **and Mengmeng Li**[1]

[1]*College of Petroleum Engineering, Xi'an Shiyou University, Xi'an 710065, China*
[2]*Shaanxi Key Laboratory of Well Stability and Fluid & Rock Mechanics in Oil and Gas Reservoirs, Xi'an Shiyou University, Xi'an, 710065, China*

Correspondence should be addressed to Gang Bi; big@xsyu.edu.cn

Received 9 October 2022; Revised 14 November 2022; Accepted 17 November 2022; Published 6 December 2022

Academic Editor: Keliu Wu

The reservoir anisotropy, perforating skin, and the compressibility of rock and fluids are important factors affecting horizontal well productivity. In this research, the finite volume method is adopted to develop a three-dimensional unsteady productivity prediction model for horizontal wells. An improved Peaceman well model is used to predict the productivity of horizontal wells. The influence of parameters, including the plane anisotropy, horizontal well length, and perforation skin on productivity were studied and the production law for horizontal wells was further analyzed. The accuracy of the model is verified by CMG reservoir simulation software. The following conclusions are obtained from study: first, the speed of pressure propagation in homogeneous and isotropic reservoir is faster than the anisotropic reservoir. Second, the flow rate of the horizontal well is U-shaped along the horizontal wellbore, and the contribution of perforation sections at both ends of horizontal wells to the total production is greater than that in the middle of horizontal wells. With the continuous production, the contribution of perforation sections at both ends gradually increases. Third, the accumulative production of a horizontal well increases with an increase in rock compressibility. The main reason is that with the increase of the elastic energy in reservoir, the accumulative production of the horizontal well under the same conditions gets higher. The proposed model can be used to predict pressure and production distribution for horizontal well in anisotropic reservoirs.

1. Introduction

Horizontal wells increase the contact area between wellbores, and improve the ultimate oil and gas recovery, which have been widely used in the petroleum engineering field nationally and internationally. Since the 1950s, scholars have conducted many in-depth studies on models for predicting horizontal well productivity [1]. The main research methods can be divided into four categories: (1) experimental simulations based on the similarity principle for hydropower; (2) analytical models; (3) semianalytical models; and (4) numerical models. Generally, a hydropower simulation can only obtain the steady-state productivity of horizontal wells in isotropic reservoirs, and experimental results are often used for qualitative analysis [2–5]. Analytical models are generally constructed based on potential function theory [6–9], and there are many assumptions in the models. Some representative models are the Giger model [10] and Joshi model [11]. Many improvements and refinements have been made to the Josh model by domestic and foreign scholars. The analytical model equation is simple and provides an important theoretical basis for early scholars to quickly understand the production law for a horizontal well. However, this model can only predict the steady-state productivity of horizontal wells. Most semianalytical models are constructed based on the theory of source functions; the source functions established by Griengaten (1973) [12] and Ozkan [13] are the most widely used. The former is mainly applied to the seepage problem for a single medium reservoir, while the latter is mainly applied to a dual medium reservoir with natural fractures. The semianalytical model can calculate the unsteady productivity of horizontal wells, which is

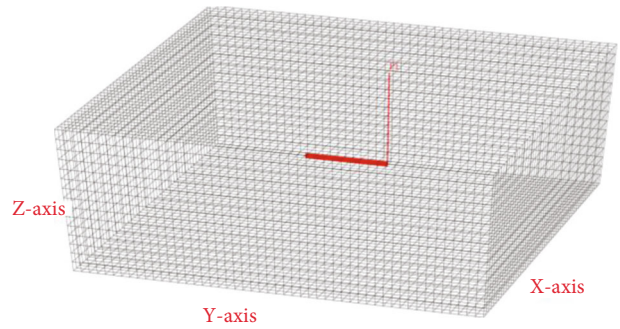

Figure 1: Schematic diagram of physical model of a horizontal well in three-dimensional box-like reservoir.

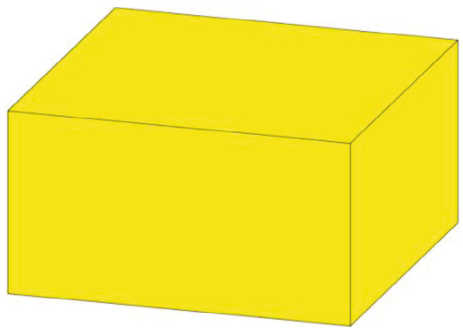

Figure 2: Arbitrary discrete element in a three-dimensional reservoir.

convenient to consider the influence of reservoir anisotropy, but it is difficult to consider the influence of negative perforation skin [14]. Comparatively speaking, so complex are the numerical modeling and solving that the model's solving ability is much higher than that of the above three methods [15–17]

The mechanical properties of porous media, providing reservoir space for fluid, have an important effect on oil well production. The early studies mainly focused on the percolation behavior of fluid in pores, while the rock matrix was regarded as a rigid percolation channel with little consideration of the mechanical properties of each system. Terzaghi [18] was the first to describe the phenomenon of coupling between solid deformation and fluid flow and put forward the concept of effective stress. Biot [19] established the three-dimensional consolidation theory by analyzing the rule for the action of the pore pressure on triaxial deformed materials. Aimed at making this theory consistent with the traditional seepage model, Geertsma [20], Verruijt [21], Chen et al. [22], and other scholars redefined and interpreted Biot's theory, and proposed the isotropic stress-seepage coupling model for a single pore. According to the references, few scholars have considered the fluid–structure coupling of porous media in anisotropic reservoirs [23–26] to establish a three-dimensional unsteady productivity model for horizontal wells.

By utilizing the finite-volume method, this paper introduces a three-dimensional unsteady productivity-prediction model developed for horizontal wells in anisotropic reservoir. The equivalent permeability and equivalent reservoir radius is used for characterizing the reservoir anisotropy. Moreover, a new porosity formula is proposed considering the rock plastic deformation. In addition, perforated skin is used to consider the effect of perforation. The influence of the reservoir anisotropy, perforation skin and horizontal well length on the production law for horizontal wells were analyzed, which provides a theoretical basis for understanding the production performance of horizontal wells.

2. Physical Model Description

The physical model of the reservoir is shown in Figure 1. A horizontal well producing at a constant rate is located at an arbitrary position in the reservoir. The reservoir permeability anisotropy takes into account the compressibility of reservoir rocks and fluids. The fluid is slightly compressible and obeys Darcy's law. It is assumed that the reservoir pressure is constant before production and that the reservoir temperature is constant during production. The influence of gravity is ignored.

3. Mathematical Model

In the productivity prediction model, the equivalent permeability and equivalent reservoir radius are calculated for reservoir anisotropy. A new porosity formula considering the plastic deformation of rock is proposed. An improved Peaceman well model is proposed for the inner boundary conditions of the model. In addition, perforated skin and rock deformation are also considered in this model, due to which the model is complicated and needs to be solved by FVM and Newton–Raphson iterative method.

The three-dimensional reservoir was separated into orthogonal grids, and the schematic diagram for any grid is shown in Figure 2.

The volume of the element body is Ω, and the external surface area of the element body is denoted as $\partial\Omega$. The lengths of the element body in the X, Y, and Z directions are $\triangle x$, $\triangle y$, and $\triangle z$.

3.1. Continuity Equation. The fluid mass conservation equation is

$$\frac{\partial}{\partial t}\int_{\Omega}\varphi\rho d\vec{x} + \int_{\partial\Omega}\rho\vec{v}\cdot\vec{n}ds = \int_{\Omega}q_w d\vec{x}. \quad (1)$$

In Equation (1), the first term on the left represents the rate of the mass change caused by the fluid density change in the unit, and the second term on the left represents the rate of the mass change caused by the fluid flow out of the unit. The right end represents the mass change caused by the source term.

In Equation. (1), φ is the porosity; ρ is the fluid density, kg/m^3; $\vec{v}$is the fluid velocity, m/s; $\vec{n}$ is the surface normal vector; and q_w is the source term, kg/s.

Table 1: Summary of basic reservoir parameters.

(a)

X Length, m	Y Length, m	Z Length, m	Porosity, %	Permeability, mD	Rock Compressibility, MPa-1
1000	1000	40	15	30	10^{-6}

(b)

Initial formation pressure, MPa	Fluid viscosity, mPa•s	Fluid density, Kg/m^3	Fluid compressibility, MPa^{-1}	Constant pressure production, MPa	Skin coefficient
1000	1000	40	15	30	10^{-6}

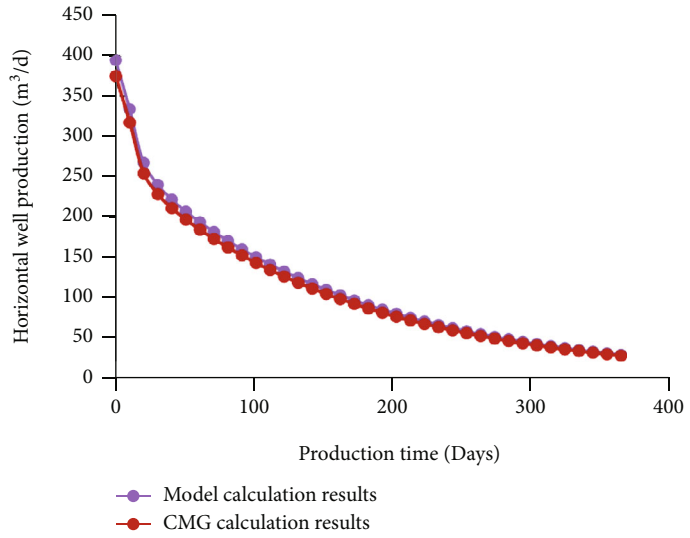

Figure 3: Comparison between the calculation results of the model and CMG software.

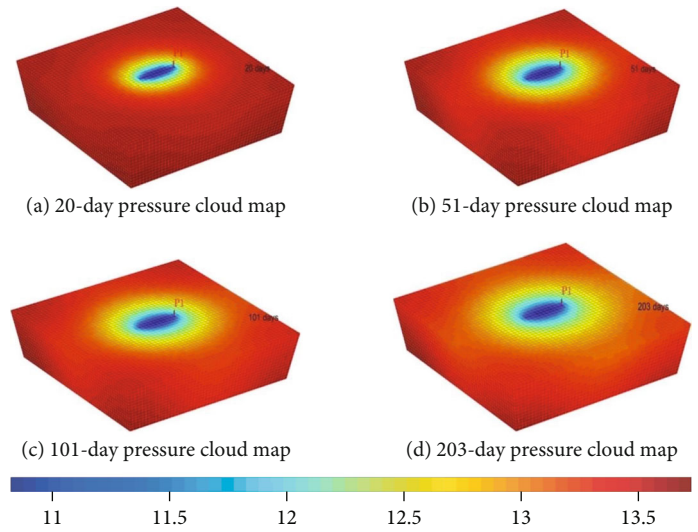

Figure 4: Pressure cloud diagram of horizontal wells in homogeneous reservoirs at different production times.

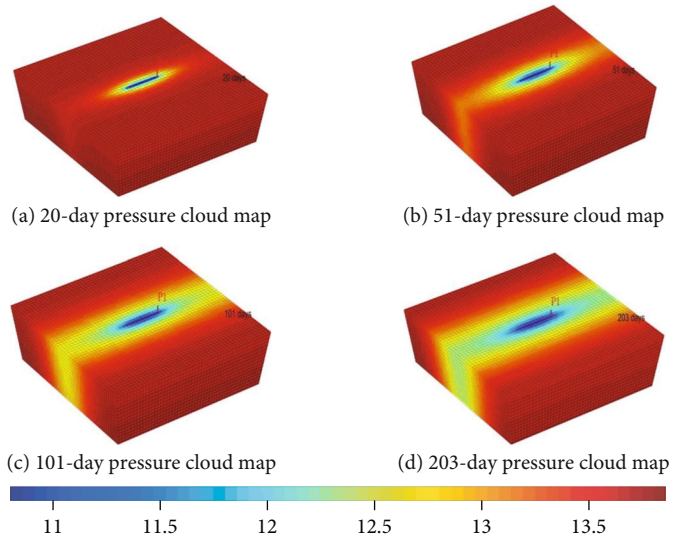

Figure 5: Pressure cloud diagram of horizontal well in anisotropic reservoir at different production times.

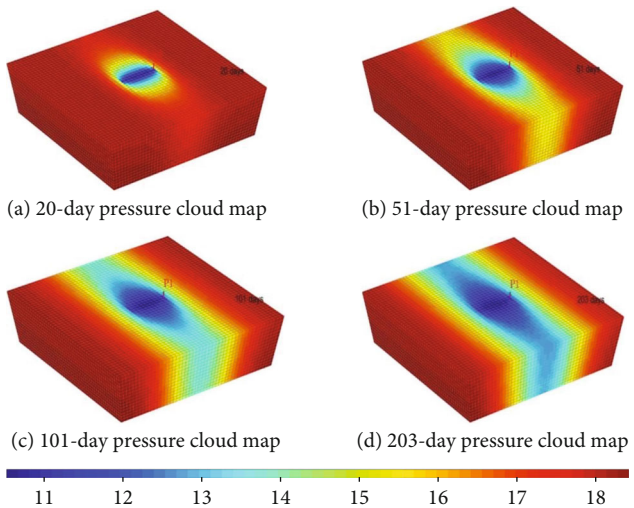

Figure 6: Pressure cloud diagram of horizontal well in anisotropic reservoir at different production times.

Based on the Gaussian divergence theorem, the above equation can be written as

$$\int_{\Omega}\left[\frac{\partial}{\partial t}\varphi\rho+\nabla\cdot\left(\rho\vec{v}\right)\right]d\vec{x}=\int_{\Omega}q_w d\vec{x}. \tag{2}$$

In Equation (2), $\nabla\cdot()$is the divergence symbol.

It can be further written as

$$\frac{\partial(\varphi\rho)}{\partial t}+\nabla\cdot\left(\rho\vec{v}\right)=q_w. \tag{3}$$

3.2. Equation of Motion. The fluid movement in the reservoir satisfies the Darcy flow equation, as shown as

$$\vec{v}=-\frac{K}{\mu}\nabla p. \tag{4}$$

In Equation (4), K is the reservoir permeability, m^{-2}; μ is the viscosity of crude oil, Pa.s; $\nabla$is the gradient symbol; P is the pressure, Pa; and g is the gravity, m/s^2.

Considering the reservoir anisotropy, the permeability is

$$K=\begin{pmatrix}K_x & 0 & 0\\ 0 & K_y & 0\\ 0 & 0 & K_z\end{pmatrix}. \tag{5}$$

3.3. Equation of State. Assuming that both the rock and fluid are weakly compressible, the relationship between the porosity, density, and pressure is as follows:

$$\varphi(p)=\varphi_0 e^{c_r(p-p_0)}. \tag{6}$$

In Equation (6), $\varphi_0$is the porosity under the reference pressure; c_r is the rock compression coefficient, pa^{-1}; and p_0 is the reference pressure, pa.

3.4. Rock Plastic Deformation. The change in the total volume of the rock and soil minus the expansion term (that is, the change in the volume of the rock and soil particles) is the change in the pore volume.

$$\Delta V_p=\Delta V_b-\Delta V_r. \tag{7}$$

In Equation (7), $\Delta V_p$is the change in the rock and soil pore volume, m^3; $\Delta V_b$is the volume change for the rock and soil, m^3; andΔV_r is the volume change for the rock and soil matrix, m.

Therefore, the new porosity is

$$\phi=\frac{V_p+(\Delta V_b-\Delta V_r)}{V_b+\Delta V_b}. \tag{8}$$

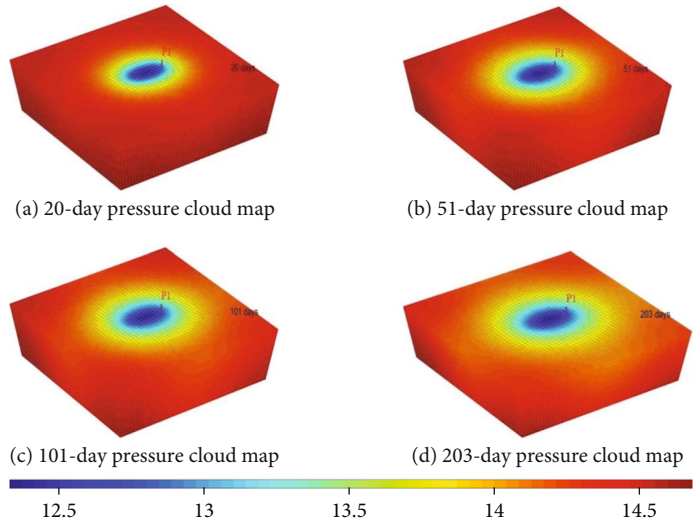

Figure 7: Pressure cloud diagram of horizontal well in anisotropic reservoir at different production times.

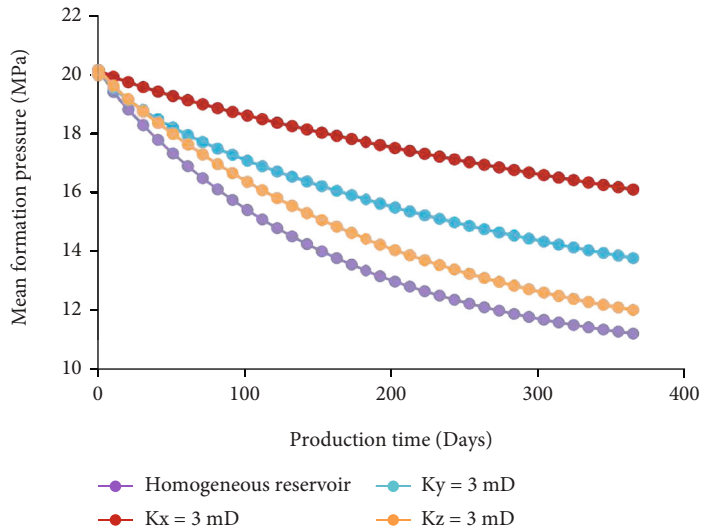

Figure 8: Variation curve for average reservoir pressure.

In Equation (8), V_p is the rock pore volume, m^3, and φ is the porosity.

The ratio of the new permeability to the original permeability is

$$\frac{K}{K_0} = \frac{\phi/k_x {S_p}^2}{\phi_0/k_x {S_{p0}}^2} = \frac{\phi {S_{p0}}^2}{\phi_0 {S_p}^2} \tag{9}$$

In Equation (9), K is the new absolute permeability, m^2; K_0 is the original permeability, m^2; S_p is the specific surface area, m^2/m^3; and S_{p0} is the original specific surface area, m^2/m^3.

3.5. Boundary Conditions. The outer boundary is a closed boundary condition

$$\vec{v} \cdot \vec{n} = 0 \; \vec{x} \in \partial\Omega. \tag{10}$$

An improved Peaceman well model is used for the inner boundary

$$q_w = \frac{K_e h}{\mu B[\ln (r_e/r_w) + S]} \left(P_e - P_{wf}\right). \tag{11}$$

In Equation (11), q_w is the flow rate of the perforating section, m^3/s; B is the volume coefficient of crude oil, m^3/m^3; K_e is the equivalent permeability, m^{-2}; h is the mesh thickness of the well, m; r_e is the equivalent reservoir radius, m; r_w is the wellbore radius, m; S is the skin coefficient; P_e is the equivalent reservoir pressure, Pa; and P_{wf} is the bottom-hole flow pressure, Pa.

For anisotropic reservoirs, the equivalent permeability is

$$K_e = \sqrt{K_x K_y}. \tag{12}$$

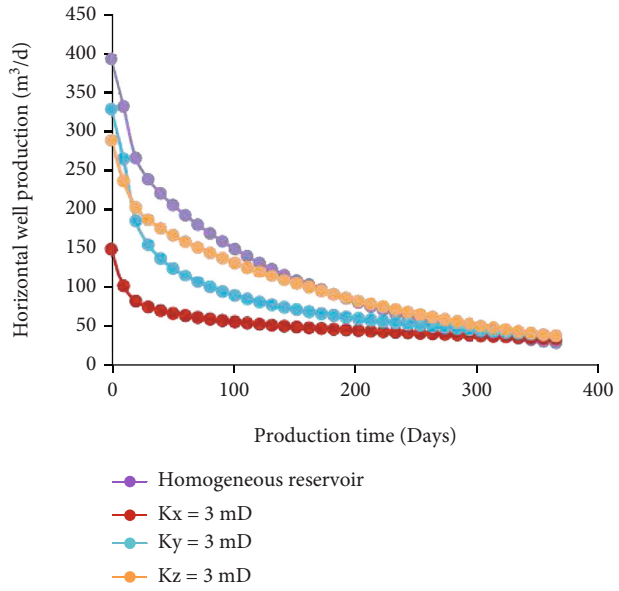

Figure 9: Daily variation curve for horizontal wells.

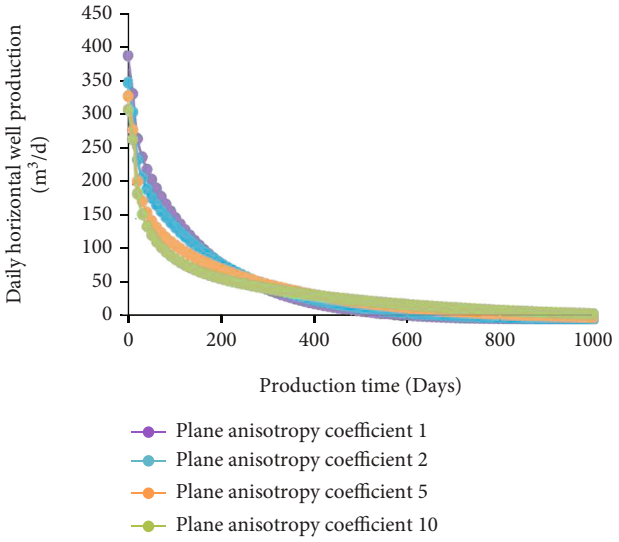

Figure 10: Horizontal well daily variation curve.

For the anisotropic horizontal well, its equivalent reservoir radius is

$$r_e = 0.28 \frac{\left\{\left[\left(K_z/K_x\right)^{1/2}(\Delta x)^2\right] + \left[\left(K_x/K_z\right)^{1/2}(\Delta z)^2\right]\right\}^{1/2}}{\left(K_z/K_x\right)^{1/4} + \left(K_x/K_z\right)^{1/4}}. \tag{13}$$

3.6. Initial Conditions. The initial reservoir pressure is equal

$$P(t=0) = P_r. \tag{14}$$

In Equation (14), P_r is the initial reservoir pressure, pa.

4. Solution of Mathematical Model

Assuming that the reservoir is separated into M units and N perforation sections, there are M + N + 1 unknowns for this physical problem, which are the flow pressure of the M units, the flow pressure of the N perforation sections, and the wellhead flow pressure, respectively. Equation (2) is simplified in conjunction with (4-6), and discretized in time, the mass conservation equation for M units is

$$\frac{P^{n+1} - P^n}{\Delta t} - \frac{1}{c_t \mu \varphi} \nabla \cdot \left(K \nabla \left(P^{n+1}\right)\right) - q_w^n = 0. \tag{15}$$

In Equation (15), the superscript n is the nth time step (known); n + 1 is the n + 1-th time step (unknown); q_w is the perforating flow rate (unknown), kg/s; and c_t is the comprehensive compression coefficient, and the expression is

$$c_t = c_r + c_f. \tag{16}$$

N equations can be obtained by using Equation (11), $M + N$ equations can be obtained by combining Equation (15), $M + N + 1$ equations can be constructed by combining with constant pressure production, the number of equations is equal to the number of unknowns, and the solution of the equations can be obtained by using the Newton–Raphson iterative method.

5. Correctness Verification and Result Analysis

5.1. Basic Reservoir Data. The three-dimensional box-shaped reservoir size was 1000 m × 1000 m × 40 m, the horizontal well length was 220 m, the horizontal well location coordinate for the x-axis was 500 m, and that for the z-axis was 20 m. The well root is located in the y-axis at 400, and the well toe is located in the y-axis at 600 m (that is, the horizontal well is located in the middle of the box-shaped reservoir). The other basic parameters of reservoirs are shown in Table 1.

5.2. Model Correctness Verification. Based on the data in Table 1, the CMG 2015 IMEX black oil module was used to verify the correctness of the model. The simulation results are shown in Figure 3. The simulation comparison results show that there is a little difference between the two models in the early stage of simulation, and the difference becomes increasingly small with the advance of production. The little difference is caused by the error of numerical method to solve the seepage equation, resulting in small errors in the results. Therefore, the model solution is basically consistent with the results of the CMG simulation.

5.3. Analysis of Pressure-Propagation Law of Horizontal Wells

5.3.1. Homogeneous Reservoir. The reservoir is an isotropic reservoir, and the basic data are shown in Table 1. When the horizontal well is in production for 20 days, 51 days, 101 days, and 203 days, the pressure cloud diagram is as shown in Figure 4. As can be observed from the figure, the

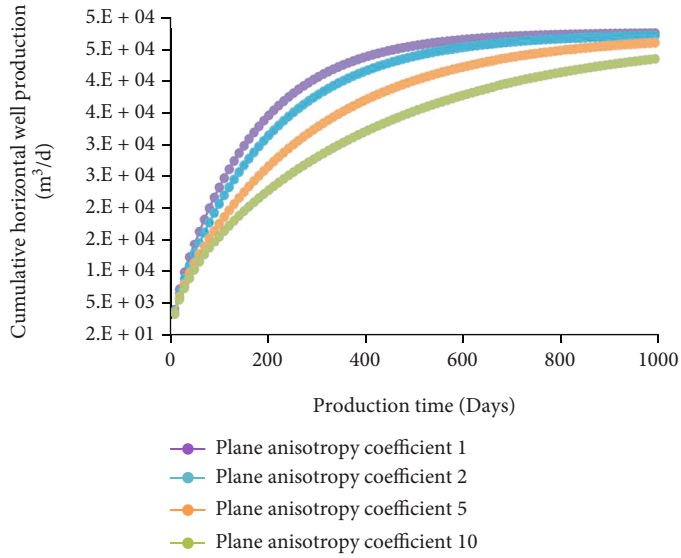

Figure 11: Variation curve for horizontal well accumulative production.

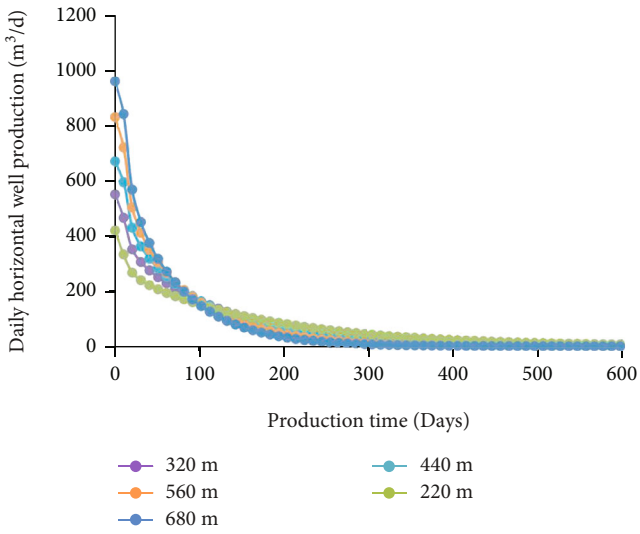

Figure 12: Horizontal well daily variation curve.

reservoir pressure spreads outwards in an elliptical shape. With the progress of production, the pressure distribution becomes more widespread, with the lowest reservoir pressures near the well area.

5.3.2. Anisotropic Reservoir when $K_x = 3$ mD. The other basic data for when $K_y = K_z = 30$ mD and $K_x = 3$ mD are shown in Table 1. The pressure cloud diagrams for horizontal wells over 20 days, 51 days, 101 days, and 203 days of production are shown in Figure 5. Compared with homogeneous reservoirs, the pressure-propagation velocity in the x-axis direction is slower and the pressure propagation in the y-axis direction is faster due to the significant decrease permeability.

5.3.3. Anisotropic Reservoir when $K_y = 3$ mD. The other basic data for when $K_x = K_z = 30$ mD and $K_y = 3$ mD are shown in Table 1. The pressure cloud diagrams of the horizontal wells at 20 days, 51 days, 101 days, and 203 days of production are shown in Figure 6. Compared with homogeneous reservoirs, the pressure-propagation velocity in the y-axis direction is slower and the pressure-propagation velocity in the x-axis direction is faster due to the significant decrease in the permeability in the y-axis direction.

5.3.4. Anisotropic Reservoir when $K_z = 3$ mD. The other basic data for when $K_x = K_y = 30$ mD and $K_z = 3$ mD are shown in Table 1. The pressure cloud diagrams for horizontal wells over 20 days, 51 days, 101 days, and 203 days of production are shown in Figure 7. The pressure propagation is similar to that for homogeneous reservoirs, but the overall pressure drop rate decreases, which can be further observed in Figure 8.

The change in the average reservoir pressure under four geological conditions is shown in Figure 8. The average formation pressure for the homogeneous reservoir shows the fastest decrease when $K_x = 3$ mD. It can also be concluded from Figure 8 that horizontal wells are more sensitive to changes in plane permeability than those in vertical permeability. In the case of anisotropic plane permeability, only when horizontal wells are arranged in the direction of the maximum plane permeability can high productivity be obtained. The above knowledge can also be obtained through the daily production curve for horizontal wells (as shown in Figure 9).

5.4. Sensitivity Analysis of Plane Anisotropy. From Section 5.2, it is clear that plane anisotropy has a great impact on horizontal well development, so K_x/K_y is defined as the plane anisotropy coefficient. Other data are shown in Table 1. When the plane anisotropy coefficient is 1, 2, 5, or 10, respectively, the variation of the daily production and cumulative production of the horizontal well is as shown in Figures 10 and 11. As shown, when horizontal wells are producing at a constant bottomhole flow pressure, the

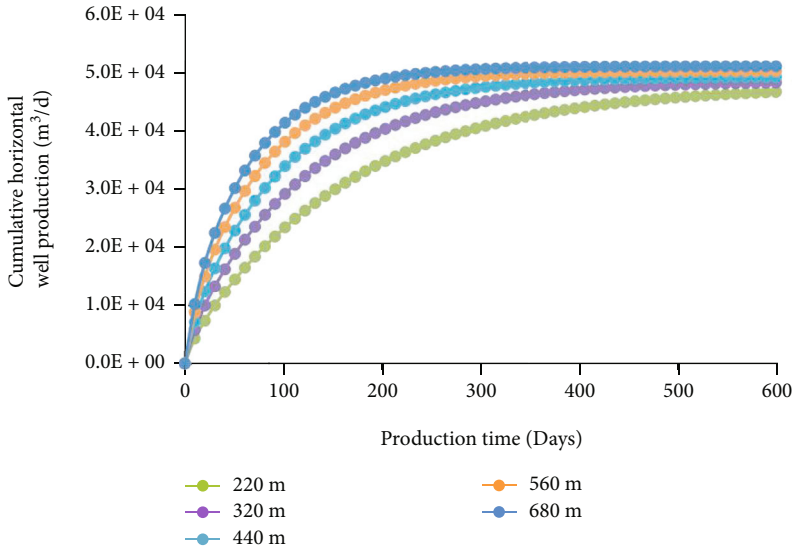

Figure 13: Variation curve for horizontal well accumulative production.

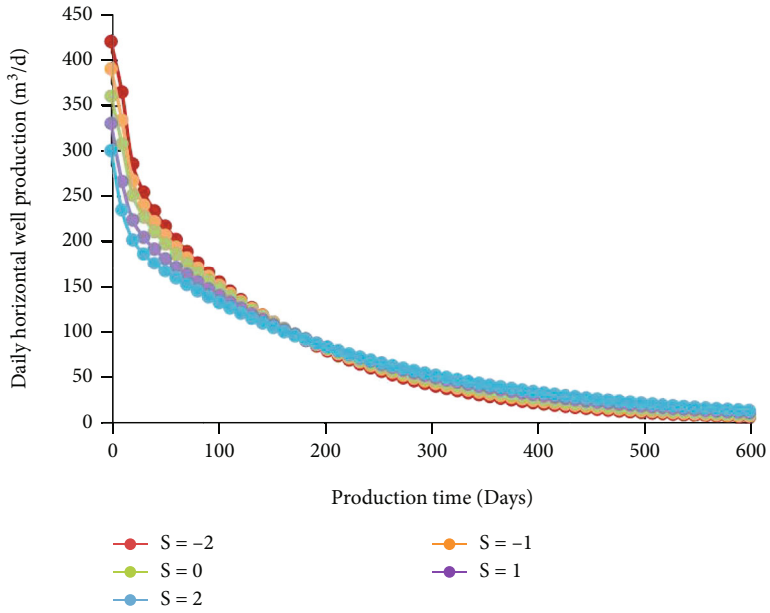

Figure 14: Daily variation curve for horizontal wells.

smaller the plane anisotropy coefficient is, the higher the initial production of horizontal wells will be, but the faster the production declines. The smaller the plane anisotropy coefficient is, the faster the accumulated production of horizontal wells will increase in the early stage, but the more slowly it will increase in the later stage.

5.5. Sensitivity Analysis of Horizontal Well Length. The other data for when the horizontal well length is 220 m, 320 m, 440 m, 560 m, and 680 m are shown in Table 1, and the cumulative production changes for horizontal wells are shown in Figures 12 and 13. It can be seen that when the horizontal well is producing at a constant bottomhole flow pressure, the length of the horizontal well is larger. The initial production of the horizontal well is higher, but the faster the production declines. The length of the horizontal well is larger, the accumulated production of the horizontal well increases faster in the early stage, and the increase in the later stage is slower.

5.6. Sensitivity Analysis for Perforation Skin. The semianalytical model for horizontal well productivity prediction is prone to erroneous results when simulating negative perforation skin. The numerical model developed in this study overcomes this shortcoming and simulates other data when the perforation skin is -2, -1, 0, 1, and 2, respectively, as shown in Table 1, and the productivity change in the horizontal well is as shown in Figures 14 and 15. It is observed that the smaller the perforating skin coefficient is, the higher the initial production of horizontal wells will be, while the

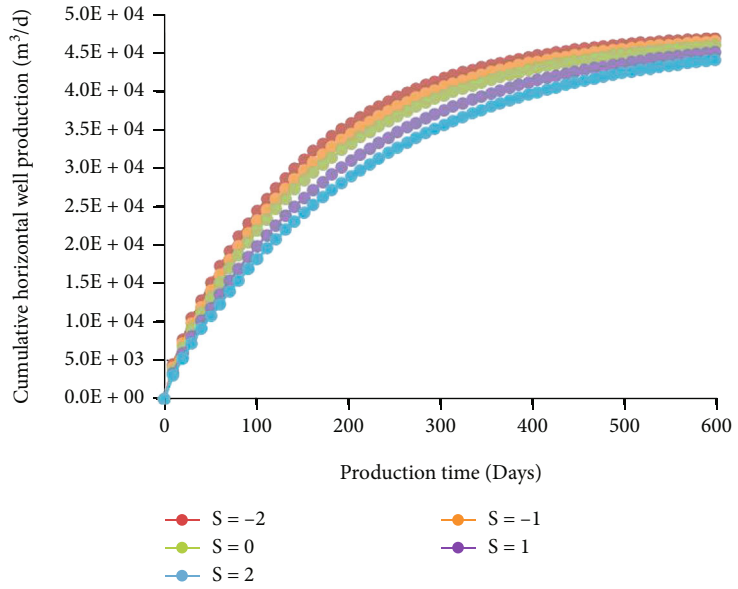

Figure 15: Variation curve for horizontal well accumulative production.

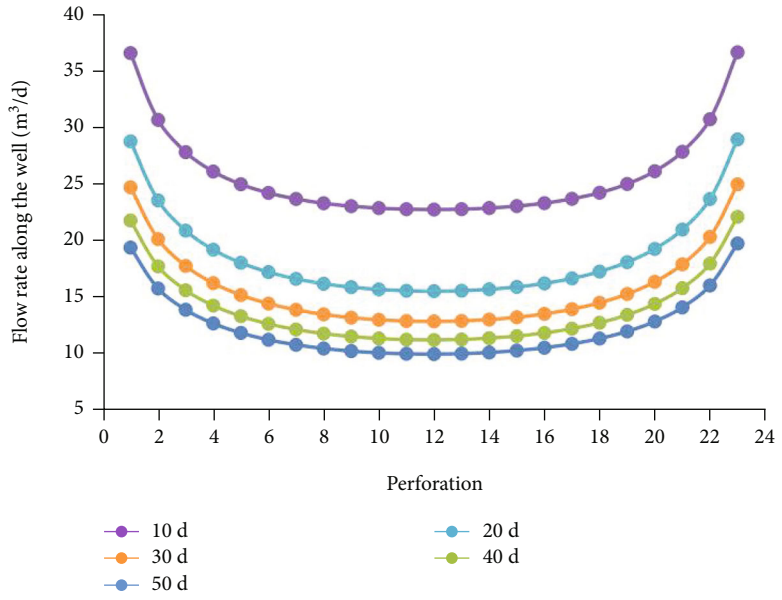

Figure 16: Variation curve for flow rate along horizontal well.

production declines faster. The smaller the perforating skin coefficient is, the faster the accumulative production of horizontal wells will increase in the early stage, and the slower the growth will increase in the later stage. The main reason is that when the perforation skin is negative, the seepage resistance for the horizontal well reduced. With the increase of the perforation skin, the discharge area gets smaller, and the production of the horizontal well becomes lower. It is an exhaustive exploitation mode for the horizontal well, therefore the production declines faster in the later stage of the production.

5.7. Analysis of Flow Rate along the Well. The horizontal well was 440 m long. Other basic data are shown in Table 1 for a total of 23 horizontal well perforations. When the horizontal well was produced for 10 days, 20 days, 30 days, 40 days, and 50 days, each perforation flow along the wellbore curve was as shown in Figure 16. It shows that, with the production continuing, the flow along the horizontal wellbore became smaller, but the magnitude of the decrease in the flow rate was gradually reduced. At different times, the 12th perforating section in the middle of the horizontal well had the lowest flow rate, while the perforating sections at both ends had

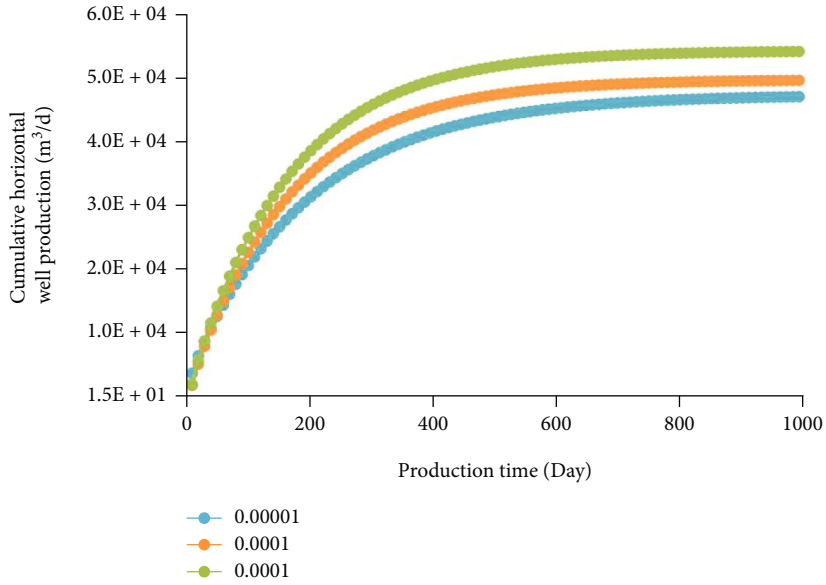

Figure 17: Variation curve for horizontal well accumulative production.

the largest flow rate. When the flow rate of the horizontal well was distributed in the U-shape along the well for 10 days, 20 days, 30 days, 40 days, and 50 days, the relative percentage differences between the maximum and minimum flow rates in the perforating section were 37.88%, 46.11%, 48.08%, 48.59%, and 48.70%, respectively, indicating that the contribution of perforating sections at both ends of horizontal wells to the total production of horizontal wells increases.

5.8. Analysis of Horizontal Well Accumulative Production. The horizontal well was 440 m long. Other basic data are shown in Table 1. When the compressibility of the rock was 10^{-3}, 10^{-4}, and 10^{-5} MPa^{-1}, respectively, the cumulative production curves for the horizontal well were as shown in Figure 17. It can be observed from Figure 17 that the accumulative production of the horizontal well increased with an increase in rock compressibility. The main reasons are the greater compressibility of the rock, the greater elastic energy of the reservoir. Under the same conditions, the accumulative production of the horizontal well is higher.

6. Conclusions

By considering the anisotropic, perforation skin, and rock plastic deformation, the finite-volume method was applied in this paper to establish a three-dimensional unsteady flow model for horizontal wells. The reservoir anisotropy is indicated by the equivalent permeability and equivalent reservoir radius. And a new porosity equation considering plastic deformation of rocks is proposed. The CMG reservoir simulation software was used to verify the correctness of the model established in this work, and the following conclusions were obtained:

(1) Through simulating the change of average reservoir pressure under four geological conditions, the average formation pressure of homogeneous reservoir has the fastest decrease and the production is the highest. When anisotropy exists in the reservoir, horizontal wells must be placed along the direction of maximum planar permeability to obtain high production

(2) When the flow rate is U-shaped along the horizontal wellbore, the contribution of perforating sections at both ends of the horizontal well is greater than that in the middle of the horizontal well. The percentage relative differences between the maximum and minimum flow rate in the perforating section are caused by the decrease of the remaining oil in the middle horizontal well and the interference between the perforated sections

(3) The initial production rate of horizontal wells gets higher and the accumulative production in the early stage increases with the decrease of the perforation skin due to the reduction of seepage resistance in horizontal well, while the increase of accumulative production grows slower in the later stage with an exhaustive exploitation mode of the horizontal well

(4) The accumulative production of a horizontal well increases with the increase of rock compressibility. The main reasons are the greater compressibility of the rock, the greater elastic energy of the reservoir, and the higher accumulative production of the horizontal well under the same conditions

Data Availability

All data, models, and code generated or used during the study appear in the submitted paper.

Conflicts of Interest

The authors declare that they have no conflicts of interest.

Acknowledgments

This study was funded by the National Natural Science Foundation of China (No.51804258 and No.52104033), Xi'an Shiyou University Graduate Innovation and Practice Ability Training Program (No. YCS22213034), and Natural Science Foundation of Shaanxi Provincial Education Department (No.22JS029).

References

[1] R. M. Butler, "The potential for horizontal wells for petroleum production," *Journal of Canadian Petroleum Technology*, vol. 28, no. 3, pp. 61–69, 1989.

[2] C. Chang-chun and W. Jun-zhi, "Experimental study of multi-branch well electrical simulation," *Petroleum Exploration and Development*, vol. 25, no. 5, pp. 62–64, 1998.

[3] H. Guo-qing, L. Xiang-fang, and W. Xiao-dong, "Experimental study of multi-branch well electrical simulation," *Natural Gas Industry*, vol. 24, no. 10, pp. 99–101, 2004.

[4] G. Ying-chun and H. Shi-jun, "Experimental study on seepage flow in near-well reservoir zone with multi-lateral wells," *Petroleum geology and recovery efficiency*, vol. 16, no. 5, pp. 95-96, 2009.

[5] X. Li-kun, H. Guo-qing, and Z. Rui, "A new approach of 3D potential distribution experiment for multi-lateral wells," *Journal of Southwest Petroleum University: Science & Technology Edition*, vol. 37, no. 1, p. 116, 2015.

[6] H. Shi-jun, C. Lin-song, and Z. Feng-lan, "Study on productivity evaluation model of plane mult-i lateral well," *Well testing*, vol. 18, no. 4, pp. 1–5, 2009.

[7] J. Xiao-fei, L. Guang-lun, S. Zhao-bo, and Y. Chuan-jin, "A new productivity equation for horizontal wells in three-dimensional anisotropic reservoirs," *Petroleum geology and recovery efficiency*, vol. 26, no. 2, pp. 113–119, 2019.

[8] W. Yan-xin, D. Chang-yin, and G. Kai-ge, "Evaluation and comparison of steady-state horizontal well productivity model," *Journal of chengde petroleum college*, vol. 19, no. 6, pp. 1–5, 2017.

[9] L. Shuai, *Research on Productivity Evaluation of Multi-Branch Wells*, Xi 'an Shiyou University, 2017.

[10] F. M. Giger, "Horizontal wells production techniques in heterogeneous reservoirs," in *Middle East Oil Technical Conference and Exhibition*, Bahrain, 1985.

[11] S. Joshi, "Augmentation of well productivity with slant and horizontal wells (includes associated papers 24547 and 25308)," *Journal of Petroleum Technology*, vol. 40, no. 6, pp. 729–739, 1988.

[12] A. C. Gringarten and H. Jr, "The use of source and green's functions in solving unsteady-flow problems in reservoirs," *Society of Petroleum Engineers Journal*, vol. 13, no. 5, pp. 285–296, 1973.

[13] E. Ozkan, R. Spe, and G. Ra, "New solutions for well-test-analysis problems: part 1-analytical considerations," *SPE Formation Evaluation*, vol. 6, no. 3, pp. 359–368, 1991.

[14] N. Ren-shi, W. Su-ran, and J. Yong-lu, "Dynamic characteristics of negative skin pressure in multi-stage fractured horizontal wells," *China science and technology paper*, vol. 10, no. 9, pp. 1027–1032, 2015.

[15] C. Lin-song, L. Chun-lan, and L. Zhao-xin, "Three-dimensional oil-water two-phase finite element numerical simulation method for horizontal wells infractured bottom water reservoir," *Petroleum Exploration and Development*, vol. 2, pp. 57–61, 1998.

[16] Z. Zhu-mei and L. Zhao-xin, "Finite element method for simulation of horizontal reservoir," *Hydrodynamics research and Progress (Series A)*, vol. 3, pp. 261–271, 1996.

[17] C. Lin-song and L. Zhao-xin, "Finite element method for two-phase flow in horizontal well," *Research and Progress in Hydrodynamics (Series A)*, vol. 3, pp. 309–315, 1995.

[18] K. Terzaghi, *Theoretical Soil Mechanics*, Wiley, New York, 1943.

[19] M. A. Biot, "General theory of three-dimensional consolidation," *Journal of Applied Physics*, vol. 12, no. 2, pp. 155–164, 1941.

[20] J. Geertsma, "The effect of fluid pressure decline on volumetric changes of porous rocks," *Transactions of American Institute of Mining, Metallurgical, and Petroleum Engineers*, vol. 210, no. 1, pp. 331–340, 1957.

[21] A. Verruijt, *Elastic Storage in Aquifers. Flow through Porous Media*, Academic Press, New York, 2014.

[22] H. Y. Chen, L. W. Teufel, and R. L. Lee, "Coupled fluid flow geomechanics in reservoir study - I," *Theory governing equations*, vol. 30752, 2015.

[23] T. Praditia, R. Helmig, and H. Hajibeygi, "Multiscale formulation for coupled flow-heat equations arising from single-phase flow in fractured geothermal reservoirs," *Computational Geosciences*, vol. 22, no. 5, pp. 1305–1322, 2018.

[24] Q. D. Zeng, J. Yao, and J. F. Shao, "Study of hydraulic fracturing in an anisotropic poroelastic medium via a hybrid EDFM-XFEM approach," *Computers and Geotechnics*, vol. 105, pp. 51–68, 2019.

[25] R. Guo-tong, J. Jia-min, and M. Y. Rami, "A Model for coupled geomechanics and multiphase flow in fractured porous media using embedded meshes," *Advances in Water Resources*, vol. 122, pp. 113–130, 2018.

[26] Y. Xia, H. Zhao-qin, Y. Jun, L. Yang, F. Dong-yan, and Z. Kai, "An efficient hydro-mechanical model for coupled multi-porosity and discrete fracture porous media," *Computational Mechanics*, vol. 62, no. 5, pp. 943–962, 2018.